Analysis and Comparison of Features and Algorithms to Classify Shoulder Movements From sEMG Signals

Diletta Rivela, Alessia Scannella, Esteban E. Pavan, Carlo A. Frigo, Paolo Belluco, and Giuseppina Gini

***Abstract*— Shoulder movements are not considered for electromyography-based pattern classification control, due to the difficulty to manufacture three-degrees-of-freedom shoulder prostheses. This paper aims at exploring the feasibility of classifying up to nine shoulder movements by processing surface electromyography signals from eight trunk muscles. Experimenting with different pattern recognition methods, two classifiers were developed, considering six different combinations of window sizes and increments, and three feature sets for each channel. Applying linear discriminant analysis the best performance was obtained on a window length of 500 ms associated to temporal increments of 62 ms. This setting yielded a 100% accuracy for recognizing four movements, and progressively degraded to 92% for nine movements. Using neural networks, higher accuracy was obtained in particular in the 9-class problem. Finally, the signals from the eight channels were analyzed in order to check the possibility to reduce the number of acquisition channels.**

***Index Terms*— Linear discriminant analysis, neural networks, pattern recognition control, sEMG, shoulder movements.**

I. Introduction

UP TO now most of the uses of electromyography (EMG) signals are for diagnostic purposes. Other applications are related to the control of mechanical systems, as prostheses. In such prosthetic applications, surface electromyography (sEMG) signals are used to detect a voluntary movement, for example closing the hand, in order to control some actuators that activate the intended movement. When more than one movement must be independently controlled, a voluntary movement must be repeated two or three times to activate a second or a third pre-coded movement of the prosthesis. To allow a real EMG based controller to be suitable for complex full arm prostheses, it is necessary to build a multiclass classifier, able to directly detect the user intention from residual muscle activity. So far little effort has been dedicated to the control system of active full-arm prosthesis. This may be due to the relatively low incidence of major upper limb amputations and to the difficulty to control a high number of degrees of freedom. Conventional strategies of prosthetic shoulder control are based on the activation of mechanical switches [1]; other methods adopt the myoelectric control by recording, during voluntary contraction, signals from residual muscles that are not physiologically involved in the execution of shoulder motions.

Usually sEMG signals from two sites (e.g. a couple of agonist/antagonist muscles) are used to control one degree of freedom. Both methods require a considerable effort to the patient in the training phase, due to the low intuitiveness of control. Training difficulties and the complexity of the control strategies are two of the major reasons of user rejection [2].

Controllers based on EMG-based pattern recognition, able to detect the user intention, can increase the acceptance of prostheses and exoskeletons. They recognize patterns from sEMG of synergistic muscles spontaneously activated in correspondence with a predefined motor task [3], [4]. Even in the case of major upper limb amputations, trunk muscles are suitable, as they are usually preserved.

Controllers are also used in the robotic assisted neurorehabilitation. A musculoskeletal model, obtained by fusing EMG data and mechanical models, is the state of the art in neurorehabilitation. Estimates of neural excitations, derived from the amplitude of sEMG, correlate to muscle force. While this approach is being developed for the legs, it is only at the beginning for upper limbs movements [5].

According to a recent survey on robotic devices for upper limb rehabilitation [6], very few systems use EMG signals as input to control the shoulder joint of an exoskeleton, both in rehabilitation and daily use. Only Kiguchi *et al.* [7] provided a prototype system using, in combination with the shoulder joints positions, the Mean Absolute Value (MAV) of the sEMG as muscle activity level to control a 2-degree-of-freedom shoulder exoskeleton.

Other robotics devices for rehabilitation help in the repeated execution of simple mechanically constrained movements; the EMG signals provide the only clinically viable method to interface the nervous system of the patient with a mechanical device. For those applications as well as for the control of full arm prosthesis the pattern recognition approach could

Manuscript received December 14, 2017; revised February 23, 2018; accepted February 25, 2018. Date of publication March 8, 2018; date of current version April 9, 2018. The associate editor coordinating the review of this paper and approving it for publication was Dr. Roozbeh Jafari. *(Corresponding author: Giuseppina Gini.)*

D. Rivela is with the Advanced Telecommunications Research Institute International, Kyoto 619-0288, Japan (e-mail: diletta.rivela@gmail.com).

A. Scannella is with GE Healthcare, 20126 Milano, Italy (e-mail: alessia.scannella@gmail.com).

E. E. Pavan, C. A. Frigo, and G. Gini are with DEIB, Politecnico di Milano, 20133 Milano, Italy (e-mail: esteban.pavan@polimi.it; carlo.frigo@polimi.it; giuseppina.gini@polimi.it).

P. Belluco is with Comune di Milano, 20121 Milan, Italy (e-mail: paolo.belluco@polimi.it).

Digital Object Identifier 10.1109/JSEN.2018.2813434

be investigated. To our best knowledge no other work has been performed by other groups to develop a pattern recognition control for the shoulder than that previously done by us [8], [9].

Aim of the current study was to experimentally verify how effectively a pattern recognition approach could classify a quite large number of shoulder movements. To this purpose we have implemented a family of classifiers using data from eight acquisition channels. We started investigating different segmentation techniques and feature extraction methods. We compared the discrimination capabilities of three different feature extraction sets, and we analyzed the classification results for 4, 5, or 9 motions. As expected, recognizing a large number of classes is a demanding task for any classifier, so the accuracy decreases when adding more classes. The best linear classifier based on Linear Discriminant Analysis (LDA) is fully presented. To improve the classification accuracy for 9 classes, a non-linear model, based on Neural Networks (NN) is then developed. Pros and cons of the two classifiers are analyzed. Finally we have investigated the possibility to reduce the number of muscles to be considered without losing classification accuracy. To this end we have examined the information content of each channel.

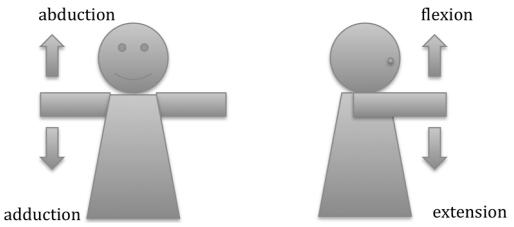

Fig. 1. Shoulder movements in the frontal and sagittal planes.

TABLE I
THE CONSIDERED CHANNELS

Electrode position	Channel
Clavicular head of the pectoralis major	1
Sternal head of the pectoralis major	2
Serratus anterior	3
Trapezius descendent	4
Trapezius transversalis	5
Trapezius ascendant	6
Infraspinatus	7
Latissimus dorsi	8

II. PATTERN RECOGNITION AND DATA SET

Myoelectric signals, when properly processed, are supposed to represent the motor command directed to the muscle actuators [10]. For controlling prostheses, the myoelectric (sEMG) signals are detected by electrodes located at the stump-socket interface, rectified and integrated in order to generate the commands that activate electric motors.

In the last decades, the use of sEMG pattern recognition for prosthetic control has been proposed and developed [2], [11]. This approach is founded on the assumption that patterns of sEMG signals from several muscles include much information about the intentional movement of the limb. The basic principle is that each sEMG pattern can be associated to one motion class among a multiplicity of preselected movements. Then the controller automatically performs the chosen movement, and the subject does not have to control each single degree of freedom. In this way, a more intuitive and rapid control can be obtained.

Generally, a pattern recognition-based control approach requires training a classifier for the intended movements starting from user's data. This approach consists of the following sequence of steps: data acquisition, data segmentation, feature extraction, feature reduction, training of the classifier, and evaluation of the classifier predictive power [12], [13].

The study here presented starts from data segmentation, since the data set used has been taken from literature, and its acquisition is fully described in [8]. The data set contains data from eight healthy subjects (four males and four females) aged 25.0 $\pm$ 1.8 years, performing eight shoulder movements: shoulder flexion at 45° , 90°, and 110°; shoulder hyperextension at $-30°$; shoulder abduction at 45° and 90°; shoulder elevation of 45° and 90° in an elevation plane externally rotated by 45° in relation to the sagittal plane. See in Figure 1 the definition of the movements.

Data were recorded at a sampling rate of 1.0 kHz from eight electrodes located on synergistic trunk muscles [14], usually preserved after upper limb amputation, as illustrated in Table 1. Standard filtering and rectification were applied to the signals.

At the beginning it is necessary to choose whether to process the full myoelectric signal, which includes transient [4], or only the part related to the steady state (i.e. during maintained contraction) signal. Steady state data are classified more accurately than transient data, and the classification suffers from less degradation with shorter data segments [15].

A crucial step is data segmentation. Since EMG is a continuous signal, it is necessary to define the time windows in order to segment it and later compute the features. Each channel is segmented into a series of time windows, adjacent or partially overlapped. The window length has to satisfy real-time constraints that require the actuation delay must not be greater than 300 ms, otherwise a movement delay will be perceived by the user [16]. For this reason, when using a window length greater than 250 ms, windows must be overlapped. However the determination of the best segmentation remains an open issue. Smith and coauthors [17] analyzed different combinations to conclude that the optimum window length for pattern recognition control is between 150 ms and 250 ms. Other researchers compared different combinations of window lengths and increments, and suggested a length of 500 ms and an increment of 125 ms [11].

After segmentation, features are computed. Generally, features belong to three main domains: time domain, frequency domain and time-frequency domain. The time domain (TD) features, based on the signal amplitude, are commonly used due to their simple definition and computation; examples for prosthesis control are presented in [18] and [19].

Feature selection may be employed to reduce the dimensionality of the initial feature space, attempting to preserve

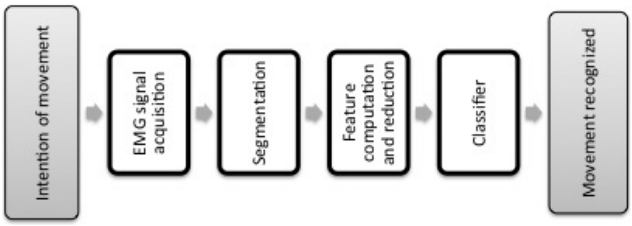

Fig. 2. The processing stages from EMG signals detection to classification output.

the classification accuracy, while reducing the computational costs and the complexity of the classifier [13]. Dimensionality reduction strategies are either feature selection or feature projection. Feature selection consists in selecting the best feature subset of the original features. Instead, in the feature projection approach, a new feature subset is created, combining the original features through a linear or non-linear mapping. Previous studies [20], [21] have shown that the projection approach leads to a higher discrimination ability compared to feature selection. According to [22] this stage plays an important role in classification accuracy, even more than the classifier itself.

The classifier to be deployed in the final system receives in real time as input the reduced feature set for each segment, and has to match the different patterns with the correct movement class. To build the classifier many choices are available, from classical statistical tools to machine learning tools. Two methods are explored in this paper, LDA and NN.

The flowchart of the processing method to construct the classifier is presented in Figure 2. Our implementation has been done in Matlab R2015a and Neural Net Toolbox (The MathWorks, Natick, USA).

III. Methods and Algorithms

A. Data Segmentation

Data analysis considered only the steady state phase (isometric hold) as in this condition the classification is more accurate [2], [15]. This phase lasted about 3 seconds.

Six signal segmentation settings were tested, by combining different window sizes (L) and increments (I): a) L = 500 ms, I = 250 ms, b) L = 500 ms, I = 125 ms, c) L = 500 ms, I = 62 ms, d) L = 250 ms, I = 250 ms, e) L = 250 ms, I = 125 ms, and f) L = 250 ms, I = 62 ms.

After a random shuffling of all acquired trials, data were split into a training dataset (the first 60%), and a test dataset (the last 40%). After feature extraction from all the datasets, the training set was used to reduce the dimensionality of the original feature set and then to train the classifier. The test dataset was only employed to estimate the classification accuracy.

B. Feature Computation and Selection

For each of the six segmentations tested, three different feature sets were extracted:

1) Hudgins' TD feature set, i.e. the mean absolute value (MAV), waveform length (WL), zero crossing (ZC), and slope sign change (SSC) [18]. Considering the 8 channels, 32 features are computed for each segment.

2) The feature vector defined in [23] containing the ZC, Willison amplitude (WAMP) and MAV features of the 2nd level reconstructed sEMG signal with 7th order Daubechies wavelet, and the MYOP feature of the 1st level reconstructed sEMG signal with 8th order Daubechies wavelet. 56 features are produced for each segment.

3) The TD feature set proposed in [11] containing the sample entropy (SampEn), cepstral coefficients (CC) of the 4th order, root mean square (RMS), and WL. 32 features for each segment are produced.

Subsequently, each feature set was reduced using the principal component analysis (PCA), as strongly suggested in [15], [16], [18], and [24]–[28]. PCA is an unsupervised method and produces a new feature set by a linear projection of the original feature vector onto the Eingenvector of the covariance matrix [29]. We kept the maximum number of principal components that make positive- definite the pooled covariance matrix. This number was 18, 56, and 24 respectively for the three feature sets, and their explained variance was 100%. We observed that without PCA the classification results sensibly degraded (up to 15%).

C. Construction of the Linear Classifier

Classification was performed using LDA [12]. This method attempts to express the dependent variable class as a linear combination of the features; it was chosen due to its advantages, as low computational cost, high-speed training, and robustness [4], [11]. Furthermore, it does not require iterative training, avoiding the potential under- or over-training, and it does not need any parameter adjustment.

The performance of the classifier was defined in terms of classification error and was evaluated by considering three different sets of motion classes.

First set – 9 classes: all the 8 motion classes described above plus the rest class;

Second set – 5 classes: shoulder flexion at 90°, shoulder hyperextension at −30°, shoulder abduction at 90°, shoulder elevation at 90° along the plane rotated by 45° in relation to the sagittal plane, and rest;

Third set – 4 classes: shoulder flexion at 90°, shoulder hyperextension at −30°, shoulder abduction at 90°, and rest.

D. Developing Non-Linear Models

The LDA classifier gave good results in accuracy; moreover it identified the combination of features that best characterizes classes through linear relationships. However LDA has been developed for normally distributed explanatory variables with equal covariance matrices, and it is difficult to know whether sEMG signals fulfill this characteristics. For this reason we developed also a NN classifier [29].

The selected architecture was a feed-forward neural network with one hidden layer. The input had 8 neurons (one for each acquisition channel), the hidden layers considered had either 20 or 50 neurons, and the output layer a neuron for each movement to classify (4, 5, or 9). The network used 3 different

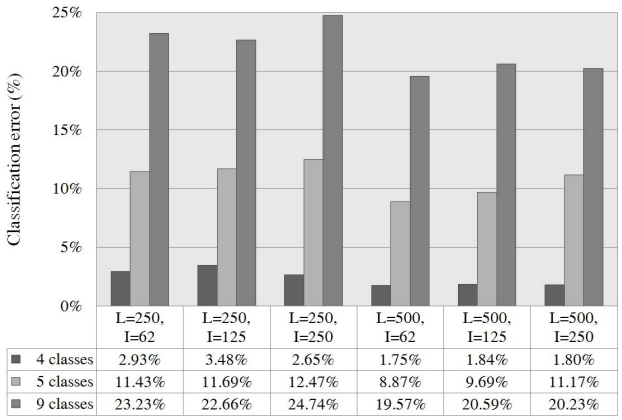

	L=250, I=62	L=250, I=125	L=250, I=250	L=500, I=62	L=500, I=125	L=500, I=250
4 classes	2.93%	3.48%	2.65%	1.75%	1.84%	1.80%
5 classes	11.43%	11.69%	12.47%	8.87%	9.69%	11.17%
9 classes	23.23%	22.66%	24.74%	19.57%	20.59%	20.23%

Fig. 3. Feature set 1 - Test classification errors (%) over all subjects, for the six different combinations of window lengths (L [ms]) and increments (I [ms]), in the four-, five- and nine- motion classes considered.

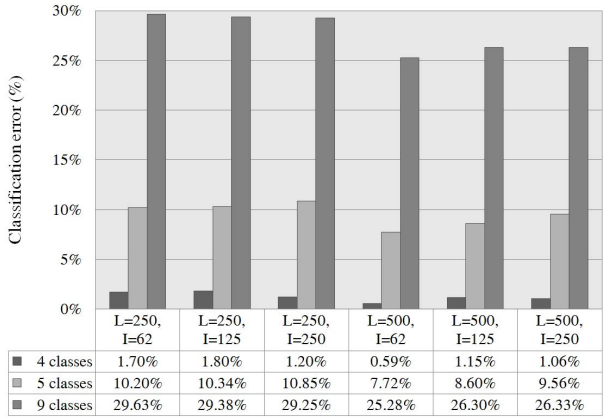

	L=250, I=62	L=250, I=125	L=250, I=250	L=500, I=62	L=500, I=125	L=500, I=250
4 classes	1.70%	1.80%	1.20%	0.59%	1.15%	1.06%
5 classes	10.20%	10.34%	10.85%	7.72%	8.60%	9.56%
9 classes	29.63%	29.38%	29.25%	25.28%	26.30%	26.33%

Fig. 4. Feature set 2 - Test classification errors (%) over all subjects, for the six different combinations of window lengths (L [ms]) and increments (I [ms]), in the four-, five- and nine- motion classes considered.

activation functions: MapMinMax in the input layer, TanH in the hidden layer, and SoftMax in the output layer. Training was backpropagation with early stopping.

E. Examining the Information of the Acquisition Channels

After having identified the best processing methods, we have investigated the effect of reducing the number of the sEMG channels on the classification performance. To this purpose, the average RMS was used as criterion of channel selection. Thus, the mean values of RMS for each motion class have been calculated for each acquisition channel, to individuate the channels with minor information content

IV. RESULTS

A. Features Sets and Classification Accuracy for the LDA Classifier

For each Feature Set analyzed, the performance of the different segmentation settings was assessed as the percentage of incorrectly classified motions over the tested motions included in each motion-classes subset considered.

1) First Feature Set: For the first feature set used, the test classification errors (%) over all subjects for each segmentation setting, considering separately the three different motion-classes, are in Fig. 3.

The best performance was obtained when windows of $L = 500$ ms were overlapped by $I = 62$ ms. For this segmentation, the errors were 1.75% to classify four motions, 8.87% for five classes, and 19.57% for nine classes. The worst performances were observed in the case of five- and nine-motion classes, using adjacent windows of length $L = 250$ ms, with an error of 12.47% and 24.74%, respectively; and, in the case of four classes, when using windows of $L = 250$ ms, $I = 125$ ms, with an error of 3.48%.

2) Second Feature Set: Fig. 4 reports the classification errors on the test set obtained from the second feature set. It can be observed that the lowest classification error was obtained for a window length $L = 500$ ms and an increment of 62 ms, which was 0.59% for the four-motion classes, while errors of 7.72% and 25.28% were observed for the

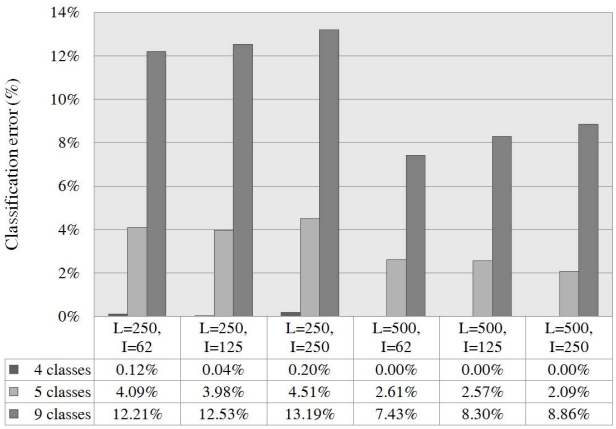

	L=250, I=62	L=250, I=125	L=250, I=250	L=500, I=62	L=500, I=125	L=500, I=250
4 classes	0.12%	0.04%	0.20%	0.00%	0.00%	0.00%
5 classes	4.09%	3.98%	4.51%	2.61%	2.57%	2.09%
9 classes	12.21%	12.53%	13.19%	7.43%	8.30%	8.86%

Fig. 5. Feature set 3 - Test classification errors (%) over all subjects, for the six different combinations of window lengths (L [ms]) and increments (I [ms]), in the four-, five- and nine- motion classes considered.

five- and nine-motion classes, respectively. On the other hand, the worst performances were: 29.63% for nine-motion classes with $L = 250$ ms and $I = 250$ ms, and a classification error of 10.85% for five classes when using $L = 250$ ms and $I = 62$ ms.

3) Third Feature Set: The test classification errors for the third feature set are in Fig. 5.

The best performance was reached for a window size $L = 500$ ms for all motion-classes subsets, and $I = 250$ ms and $I = 62$ ms for five- and nine- motion classes, respectively. For these segmentations, the classification error was 0% for four-motion classes, 2.09% for five-motion classes, and 7.44% for nine-motion classes. The worst performance was obtained using adjacent windows of $L = 250$ ms when an error of 13.19% and 4.51% was observed for nine- and five-classes, respectively.

As expected deterioration in the classification accuracy was observed when increasing the number of classes. Moreover, the classification error was affected by the segmentation settings. Taking into account the segmentation parameters that exhibited the best results from all the processing methods,

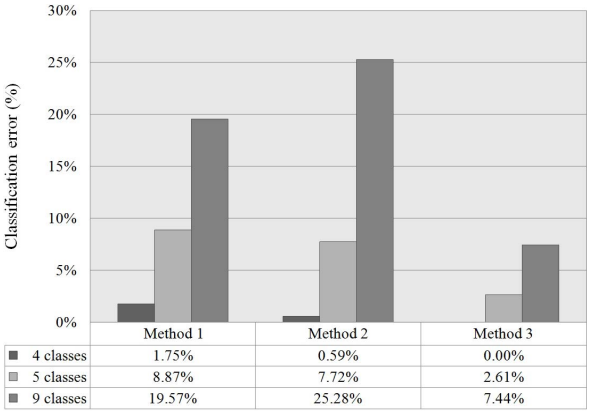

Fig. 6. Comparison of test classification errors in the three processing methods, for the best performing segmentation (L = 500 ms, I = 62 ms).

TABLE II

CONFUSION MATRIX SHOWING THE DISTRIBUTION OF ERRORS FOR THE FIVE-CLASSES PROBLEM FROM FEATURE SET 3

		True class				
		Rest	Flex. 90°	Hyp.-30°	Abd. 90°	Elev. 90°
Estimated class	Rest	100.0%	0.0%	0.0%	0.0%	0.0%
	Flex. 90°	0.0%	96.1%	0.0%	0.0%	2.3%
	Hyp.-30°	0.0%	0.0%	100.0%	0.0%	0.0%
	Abd. 90°	0.0%	0.0%	0.0%	97.2%	4.3%
	Elev. 90°	0.0%	3.9%	0.0%	2.8%	93.4%

i.e. $L = 500$ ms, $I = 62$ ms (Fig. 6), it can be seen that the third feature set yielded always the lower error. In particular, for the four-motion classes problem, the accuracy was 100%, which means that all classes were correctly classified.

This is better explained by the confusion matrices related to this last method for the classes analyzed: the values in the main diagonal are correct classifications (accuracy), and those lying outside are incorrect classifications (error rate).

For five classes the confusion matrix is reported in Table II. It can be observed that the most misclassified class was the shoulder elevation of 90° in an elevation plane externally rotated by 45°, with a classification accuracy of 93.42%, confused with abduction at 90° (4.28%) and flexion at 90° (2.30%). Instead, resting and hyperextension at −30° achieved an accuracy of 100%.

For the nine-class problem hyperextension at −30° and rest are correctly classified with 100% accuracy. The worst performance with a classification accuracy of 78.2%, is flexion at 110°, which was misclassified as flexion at 90° (14.4%) and as shoulder elevation of 90° (7.3%).

B. Accuracy of the NN Classifier

Considering that the training of neural nets improves with the number of examples, we made a different split of the sEMG data. Taking all the data of the 8 subjects and randomly extracting 70% as training set, 15% as validation set, and 15% as testing set we trained the networks and considered their predictions on the test set. Figure 7 compares the classification error of the LDA and the NN classifiers in the 9-class problem. Both for LDA and NN classifiers the higher errors are for windows of 250 ms.

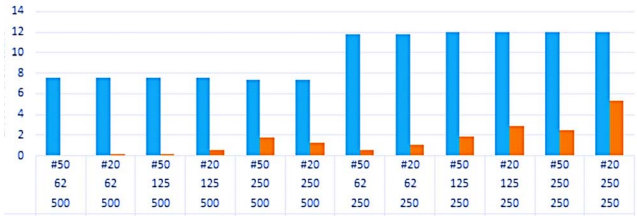

Fig. 7. Comparison of the error percentages using LDA and NN classifiers on 9 classes. In blue the percentage error for LDA, in orange for NN. We split each combination of window size and increment to show the results with #20 or #50 neurons in the hidden layer-.

TABLE III

PERCENTAGE ERROR FOR CLASSIFYING 9 CLASSES WITH NN

Window(ms)	Increment(ms)	Error%	Hidden neurons
500	62	0.08	50
500	62	0.15	20
500	125	0.2	50
500	125	0.6	20
500	250	1.76	50
500	250	1.27	20
250	62	0.57	50
250	62	1.13	20
250	125	1.85	50
250	125	2.89	20
250	250	2.47	50
250	250	5.29	20

Numerical details about the classification errors for NN are in Table III for the 9–class problem.

About the window size, we observe that the LDA classifier has a significant degradation in the accuracy when moving from the window size of 500 ms to 250 ms. In the NN the degradation is lower, so also windows of 250 ms and 62 ms increment have an acceptable error of about 1%. For 9 classes the results of NN are clearly superior: for LDA the error is about 8% while for NN it drops to 0.1%.

As performed for LDA, we built also the classifier for a reduced number of classes. We show the errors with 5 classes in Table IV.

As expected there is a significant improvement in accuracy when reducing the number of classes. While the percentage error for 5 classes in the LDA model is about 2.6%, in the NN classifier the error can drop to zero. The improvement is stronger with 4 classes, as reported in Table V.

For 4 classes, windows of 500 ms with any increment are the best ones for LDA, giving no error, while the results of NN do not depend on the windows length. For 4 classes both the LDA and the NN classifiers are almost perfect. Instead, when the number of classes increases the NN classifier shows higher performance.

TABLE IV
PERCENTAGE ERROR FOR CLASSIFYING 5 CLASSES WITH NN

Window (ms)	Increment (ms)	Error% NN	Hidden neurons
500	62	0.05	50
500	62	0.05	20
500	125	0.0	50
500	125	0.1	20
500	250	0.0	50
500	250	2.02	20
250	62	0.23	50
250	62	0.33	20
250	125	0.47	50
250	125	1.03	20
250	250	0.55	50
250	250	1.46	20

TABLE V
PERCENTAGE ERROR FOR CLASSIFYING 4 CLASSES WITH NN

Window (ms)	Increment (ms)	Error% NN	Hidden neurons
500	62	0	50
500	62	0	20
500	125	0	50
500	125	0	20
500	250	0	50
500	250	0	20
250	62	0	50
250	62	0	20
250	125	0	50
250	125	0	20
250	250	0	50
250	250	0	20

About the network architecture, we found that the number of neurons in the hidden layer is not relevant. For 5 classes, 50 hidden neurons are slightly better than 20. For the other cases, using 20 or 50 neurons does not affect the error, unless for the unlikely combination (250, 250). In conclusion, the simpler net with 20 neurons is recommended.

It is important to that when training a new net the weights are randomly initialized; it means that the accuracy can change of about $+/-$ 0.5%. All the numbers shown are obtained averaging the results of 5 trained nets.

While the performance of the NN is always superior to the performance of LDA, some considerations about using NN should be added. In particular, we cannot be sure that we construct the best classifier in one shot, and it is recommended to train more networks to select the best one. Moreover, the best property of the LDA classifier, i.e. that the boundaries between classes are at the maximum distance, is no more guaranteed for the NN classifier.

C. Reducing the Number of Channels

The best LDA classifier has been considered for the channel reduction test. Fig. 8 displays the mean values of RMS for each motion class, varying the acquisition channel for all eight subjects. The channels that show the lowest dispersion of averaged RMS among classes are: the sternal head of the pectoralis major (Ch 2) and the latissimus dorsi (Ch 8).

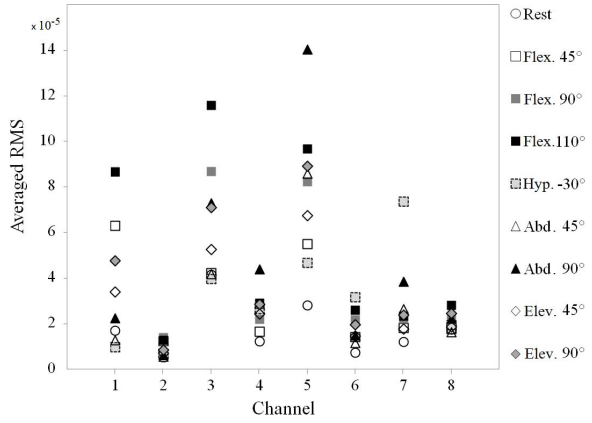

Fig. 8. Averaged RMS for each motion class, as a function of the acquisition channel (muscle) for all subjects.

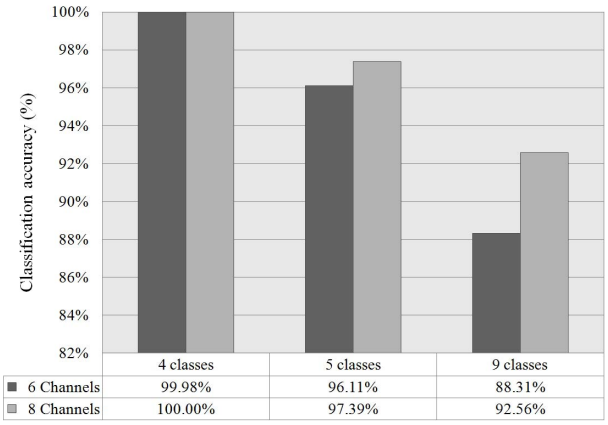

Fig. 9. Comparison of the LDA classification accuracy (%), on the test set, relative to different number of classes over all eight subjects in correspondence to the best segmentation (L = 500 ms, I = 62 ms), using 6 channels (dark grey) and 8 channels (light grey).

Thus, these channels have been removed and the same processing method for the LDA classifier has been reapplied, obtaining the results in Fig. 9.

Comparing the six-channel classifier with the eight-channel one, it can be observed that for the four-class and five-class problem, the channel reduction lead to a slight decline of classification accuracy (0.02% and 1.28%, respectively). For the nine-class problem, the classification accuracy using 6 channels suffers a significant deterioration (4.25%). Those observations suggest that for more than 5 motions only the NN model could allow the reduction of channels without losing too much in accuracy.

V. DISCUSSION AND CONCLUSION

In literature, many solutions have been developed for upper-limb prosthetic control systems based on the myoelectric signal. Much less solutions exist for the control of exoskeletons of the arm. Looking at them, only the most common levels of amputation, i.e. transradial and transhumeral levels, have been so far extensively considered.

The present work, instead, took into account the shoulder, a joint only initially studied for a possible EMG control.

Our primary aim was to develop a sEMG classification system able to correctly estimate the intentional movement of a subject within a set of motion classes, at shoulder level.

We considered different studies, which were aimed at determining the optimal window size for pattern recognition-based myoelectric control. Starting with a linear classifier, the results of our direct comparison among six different segmentation settings (as in Fig. 4, Fig. 5, and Fig. 6) showed that the best classification accuracy was reached by selecting a window length $L = 500$ ms and an interval $I = 62$ ms. The same segmentations were compared in [11] for a lower amputation level, displaying that the most suitable segmentation was instead the overlapped window with $L = 500$ ms, $I = 125$ ms. Several previous works investigated how the classification error decreases with the increase of window size [4], [17]. Indeed, choosing a greater window length, the amount of temporal information used to identify the motion class increases and the variance in the estimation of features decreases. On the other hand, a greater window length leads to a higher computational time. The combination $L = 500$ ms, $I = 62$ ms allows to obtain a decisional flow every 62 ms; this is the maximum time within which the processor must process the myoelectric signals from the eight acquisition channels and must provide output commands to the mechanical device.

Feature extraction plays an important role in the pattern recognition-based control system. Indeed, a large number of previous papers investigated which feature set returns the best classification performance, mainly for transradial and transhumeral amputation level. In this study, we have chosen three feature sets among the ones proposed in the previous works that proved to produce the lower classification error. When applied to the shoulder disarticulation problem, our results showed that the feature set composed by SampEn, CC, RMS and WL outperforms the other two feature extraction methods considered. The advantages of this feature vector are its temporal robustness, as demonstrated in [11], and its definition in time domain, which results into an easy implementation.

Table II and Table III enable to make some observations about the LDA classifier. In the 4-class problem all of the movements are correctly classified. The addition of the elevation to 90° along the inclined plane, in the 5-class problem, yields an accuracy reduction equal to 2.61%, due to the misclassification with the flexion to 90° and the abduction to 90°. This result can be explained by the fact that this movement was a combination of the two classes just mentioned. Finally, in the 9-class problem, the classification accuracy further decreases to 92.56%. This value was mainly due to the misclassification of the flexion to 110° with the flexion to 90°. This confusion can be ascribed to the closeness between these two motion classes. The accuracy significantly improves when using the NN classifier, at the cost of losing some formal properties of LDA and requiring more experience in building and maintaining the classifier.

Furthermore, when reducing the sEMG channels from eight to six, the results of the LDA classifier indicate that after removing the signals with the less discriminating information, in the four- and the five-classes problem the classification accuracy has a slight decline, while for nine movements this reduction is significant. Indeed, the more the classes of movement to be discriminated, the higher the number of acquisition channels that is required. Therefore, in the 4- and 5-class problems, only six of the eight channels can be used without compromising the classification accuracy and reducing the complexity, the weight, and the cost of the prosthesis.

Analysis of time performance of the method indicated that the most demanding feature to compute is the SampEn; the fast method proposed in [30] takes 35 ms to compute it. The computation of the full set of Phinyomark features, using Matlab on a PC requires about 1 second for a segment of 500 ms. The time required can be reduced by using a hardware-optimized implementation.

In a future work, applications of our classification approach will be explored for neuroprostheses development, i.e. for controlling Functional Electrical Stimulation based systems [31], [32], for controlling rehabilitation robotics or exoskeletons [3], as well as in the field of domotic systems, for assisting severely disabled persons.

The sEMG raw data are freely available in [33].

REFERENCES

[1] C. A. Frigo and E. E. Pavan, "Prosthetic and orthotic devices," in *Handbook of Research on Biomedical Engineering Education and Advanced Bioengineering Learning: Interdisciplinary Concepts*, Hershey, PA, USA: IGI Global, 2012, pp. 788–852.

[2] K. Englehart and B. Hudgins, "A robust, real-time control scheme for multifunction myoelectric control," *IEEE Trans. Biomed. Eng.*, vol. 50, no. 7, pp. 848–854, Jun. 2003.

[3] G. Gini, M. Arvetti, I. Somlai, and M. Folgheraiter, "Acquisition and analysis of EMG signals to recognize multiple hand movements for prosthetic applications," *Appl. Bionics Biomechanics*, vol. 9, no. 2, pp. 145–155, 2012.

[4] G. Li, "Electromyography pattern-recognition-based control of powered multifunctional upper-limb prostheses," in *Advances in Applied Electromyography*. Rijeka, Croatia: InTech Europe, 2011. [Online]. Available: http://www.intechopen.com

[5] B. Bolsterlee, D. H. E. J. Veeger, and E. K. Chadwick, "Clinical applications of musculoskeletal modelling for the shoulder and upper limb," *Med. Biol. Eng. Comput.*, vol. 51, no. 9, pp. 953–963, 2013.

[6] P. Maciejasz, J. Eschweiler, K. Gerlach-Hahn, A. Jansen-Troy, and S. Leonhardt, "A survey on robotic devices for upper limb rehabilitation," *J. Neuro Eng. Rehabil.*, vol. 11, Jan. 2014, Art. no. 3.

[7] K. Kiguchi, K. Iwami, M. Yasuda, K. Watanabe, and T. Fukuda, "An exoskeletal robot for human shoulder joint motion assist," *IEEE/ASME Trans. Mechatron.*, vol. 8, no. 1, pp. 125–135, Mar. 2003.

[8] D. Rivela, A, Scannella, E. E. Pavan, C. A. Frigo, P. Belluco, and G. Gini, "Processing of surface EMG through pattern recognition techniques aimed at classifying shoulder joint movements," in *Proc. 37th Annu. Int. Conf. IEEE Eng. Med. Biol. Soc.*, Aug. 2015, pp. 2107–2110.

[9] G. Gini, P. Belluco, F. Mutti, D. Rivela, A. Scannella, "Towards a natural interface for the control of a whole arm prosthesis," in *New Trends in Medical and Service Robots*, H. Bleuler, M. Bouri, F. Mondada, D. Pisla, A. Rodic, and P. Helmer, Eds. Cham, Switzerland: Springer, 2016, pp. 47–59.

[10] C. Frigo, M. Ferrarin, W. Frasson, E. Pavan, and R. Thorsen, "EMG signals detection and processing for on-line control of functional electrical stimulation," *J. Electromyogr. Kinesiol.*, vol. 10, no. 5, pp. 351–360, 2000.

[11] A. Phinyomark, F. Quaine, S. Charbonnier, C. Serviere, F. Tarpin-Bernard, and Y. Laurillau, "EMG feature evaluation for improving myoelectric pattern recognition robustness," *Expert Syst. Appl.*, vol. 40, no. 12, pp. 4832–4840, 2013.

[12] J. T. Tou, and R. C. Gonzalez, *Pattern Recognition Principles*. Reading, MA, USA: Addison-Wesley, 1974.

[13] A. K. Jain, R. P. W. Duin, and J. C. Mao, "Statistical pattern recognition: A review," *IEEE Trans. Pattern Anal. Mach. Intell.*, vol. 22, no. 1, pp. 4–37, Jan. 2000.

[14] M. Barbero, R. Merletti, and A. Rainoldi, *Atlas of Muscle Innervation Zones*. Milan, Italy: Springer, 2012, pp. 103–120.

[15] K. Englehart, B. Hudgin, and P. A. Parker, "A wavelet-based continuous classification scheme for multifunction myoelectric control," *IEEE Trans. Biomed. Eng.*, vol. 48, no. 3, pp. 302–311, Mar. 2001.

[16] M. A. Oskoei and H. Hu, "Myoelectric control systems—A survey," *Biomed. Signal Process. Control*, vol. 2, no. 4, pp. 275–294, 2007.

[17] L. H. Smith, L. J. Hargrove, B. A. Lock, and T. A. Kuiken, "Determining the optimal window length for pattern recognition-based myoelectric control: Balancing the competing effects of classification error and controller delay," *IEEE Trans. Neural Syst. Rehabil. Eng.*, vol. 19, no. 2, pp. 186–192, Apr. 2011.

[18] B. Hudgins, P. Parker, and R. N. Scott, "A new strategy for multifunction myoelectric control," *IEEE Trans. Biomed. Eng.*, vol. 40, no. 1, pp. 82–94, Jan. 1993.

[19] M. A. Oskoei and H. Hu, "Support vector machine-based classification scheme for myoelectric control applied to upper limb," *IEEE Trans. Biomed. Eng.*, vol. 55, no. 8, pp. 1956–1965, Aug. 2008.

[20] T. A. Kuiken *et al.*, "Targeted muscle reinnervation for real-time myoelectric control of multifunction artificial arms," *J. Amer. Med. Assoc.*, vol. 301, pp. 619–628, Feb. 2009.

[21] P. Kaufmann, K. Englehart, and M. Platzner, "Fluctuating EMG signals: Investigating long-term effects of pattern matching algorithms," in *Proc. 32nd Annu. Int. Conf. IEEE EMBC*, Buenos Aires, Argentina, Aug./Sep. 2010, pp. 6357–6360.

[22] L. Hargrove, Y. Losier, B. Lock, K. Englehart, and B. Hudgins, "A real-time pattern recognition based myoelectric control usability study implemented in a virtual environment," in *Proc. 29th Annu. Int. Conf. IEEE EMBS*, Lyon, France, Aug. 2007, pp. 4842–4845.

[23] A. Phinyomark, A. Nuidod, P. Phukpattaranont, and C. Limsakul, "Feature extraction and reduction of wavelet transform coefficients for EMG pattern classification," *Electron. Elect. Eng.*, vol. 122, no. 6, pp. 27–32, 2012.

[24] K. Englehart, B. Hudgins, P. A. Parker, and M. Stevenson, "Classification of the myoelectric signal using time-frequency based representations," *Med. Eng. Phys.*, vol. 21, nos. 6–7, pp. 431–438, 1999.

[25] G. G. Yen and K.-C. Lin, "Wavelet packet feature extraction for vibration monitoring," *IEEE Trans. Ind. Electron.*, vol. 47, no. 3, pp. 650–667, Jun. 2000.

[26] Y. Huang, K. B. Englehart, B. Hudgins, and A. D. C. Chan, "A Gaussian mixture model based classification scheme for myoelectric control of powered upper limb prostheses," *IEEE Trans. Biomed. Eng.*, vol. 52, no. 11, pp. 1801–1811, Nov. 2005.

[27] G. Wang, Z. Wang, W. Chen, and J. Zhuang, "Classification of surface EMG signals using optimal wavelet packet method based on Davies-Bouldin criterion," *Med. Biol. Eng. Comput.*, vol. 44, no. 10, pp. 865–872, 2006.

[28] L. J. Hargrove, G. Li, K. B. Englehart, and B. S. Hudgins, "Principal components analysis preprocessing for improved classification accuracies in pattern-recognition-based myoelectric control," *IEEE Trans. Biomed. Eng.*, vol. 56, no. 5, pp. 1407–1414, May 2009.

[29] C. M. Bishop, *Neural Networks for Pattern Recognition*. New York, NY, USA: Oxford Univ. Press, 1996.

[30] Y.-H. Pan, Y.-H. Wang, S.-F. Liang, and K.-T. Lee, "Fast computation of sample entropy and approximate entropy in biomedicine," *Comput. Methods Programs Biomed.*, vol. 104, no. 3, pp. 382–396, 2011.

[31] M. Ferrarin, E. E. Pavan, R. Spadone, R. Cardini, and C. Frigo, "Standing-up exerciser based on functional electrical stimulation and body weight relief," *Med. Biol. Eng. Comput.*, vol. 40, no. 3, pp. 282–289, 2002.

[32] R. Riener, M. Ferrarin, E. E. Pavan, and C. A. Frigo, "Patient-driven control of FES-supported standing up and sitting down: Experimental results," *IEEE Trans. Rehabil. Eng.*, vol. 8, no. 4, pp. 523–529, Dec. 2000.

[33] G. Gini, E. Pavan, C. Frigo, D. Rivela, A. Scannella, and P. Belluco. *sEMG Shoulder Mendeley Data*. Accessed: Mar. 1, 2018. [Online]. Available: http://dx.doi.org/10.17632/sfw6rzdjdf.1

Diletta Rivela was born in Palermo, Italy, in 1988. She received the B.S. degree in biomedical engineering from the Politecnico di Milano, Milan, Italy, in 2010, and the M.S. degree in electronic technologies from the Politecnico di Milano, Milan, Italy, in 2013. She is currently a Research Associate with the Advanced Telecommunications Research Institute International, Kyoto, Japan.

Alessia Scannella received the B.S. and M.S. degrees in biomedical engineering from the Politecnico di Milano, Milan, Italy, in 2010 and 2013, respectively. She is currently the Service Delivery Leader with GE Healthcare, Milano, Italy.

Esteban E. Pavan received the M.D. degree in electronic engineering and the Ph.D. degree in biomedical engineering from the Politecnico di Milan, Italy, in 2003. He is a Coordinator of the Movement Biomechanics and Motor Control Laboratory, DEIB, Politecnico di Milano. His main research projects include human movement analysis, biomechanics of prostheses, and orthoses and modeling of the skeletal muscle system. He is a member of the Italian Society of Clinical Movement Analysis and the Italian National Group of Bioengineering.

Carlo A. Frigo is an Associate Professor with the Politecnico di Milano, teaching bioengineering of motor system and motor rehabilitation. He is the Past President of the Italian Society for Clinical Movement Analysis, served in several research projects and in the organization of scientific events. His interests include human movement analysis, biomechanics, motor control and musculoskeletal modeling. In 2012, he delivered the invited Baumann Lecture at the Congress of the European Society for Movement Analysis in Adults and Children.

Paolo Belluco received the M.Sc. degree in computer science engineering and the Ph.D. degree in mechanics from the Politecnico di Milano, Italy, in 2006 and 2011, respectively. He was a Research Fellow with the Artificial Intelligence and Robotics Laboratory, Politecnico di Milano. He is a registered Professional Engineer. His current interests include biological signal processing for wearable applications.

Giuseppina Gini received the Doctoral degree in physics from the Milano University and specialized in artificial intelligence at the Politecnico di Milano and Stanford University. Since 1987, she has been an Associate Professor of Robotics with the Politecnico di Milano. Her research interests are humanoid robotics, sensor-based systems, cognitive systems, and pattern recognition. She directed about 20 International projects on the above topics.